PROCEEDINGS OF SPIE

OCD enhanced: implementation and validation of spectral interferometry for nanosheet inner spacer indentation

Schmidt, D., Durfee, C., Pancharatnam, S., Medikonda, M., Greene, A., et al.

SPIE.

OCD enhanced: Implementation and Validation of Spectral Interferometry for Nanosheet Inner Spacer Indentation

D. Schmidt[a,*], C. Durfee[a], S. Pancharatnam[a], M. Medikonda[a], A. Greene[a], J. Frougier[a], A. Cepler[b], G. Belkin[c], D. Shafir[c], R. Koret[c], R. Shtainman[c], I. Turovets[c], S. Wolfling[c]

[a]IBM Research, 257 Fuller Road, Albany, NY, USA 12203
[b]Nova Measuring Instruments Inc, 3342 Gateway Blvd, Fremont, CA, USA 93117
[c]Nova Measuring Instruments Ltd, 5 David Fikes St, Rehovot, Israel 7610201

*schmidt@ibm.com

ABSTRACT

In this work, the novel enhancement to multichannel scatterometry data collection, Spectral Interferometry, is introduced and discussed. The Spectral Interferometry technology adds unique spectroscopic data by providing absolute phase information. This enhances metrology performance by improving sensitivity to weak target parameters and reducing parameter correlations. Spectral Interferometry enhanced OCD capabilities were demonstrated for one of the most critical and challenging applications of gate-all-around nanosheet device manufacturing: lateral etching of SiGe nanosheet layers to form inner spacer indentations. The inner spacer protects the channel from the source/drain regions during channel release and defines the gate length of the device. Additionally, a methodology is presented, which enables reliable and reproducible manufacturing of reference samples with engineered sheet-specific indent variations at nominal etch processing. Such samples are ideal candidates for evaluating metrology solutions with minimal destructive reference metrology costs. Two strategies, single parameter and sheet-specific indent monitoring are discussed, and it was found that the addition of spectroscopic information acquired by Spectral Interferometry improved both optical metrology solutions. In addition to improving the match to references for single parameter indent monitoring, excellent sheet-specific indent results can be delivered.

Keywords: OCD, Spectral Reflectometry, Spectral Interferometry, gate-all-around, nanosheet FET, indent, inner spacer

1. INTRODUCTION

Over the last few decades, optical critical dimension (OCD) metrology has played a pivotal role in the semiconductor manufacturing process due to its extreme sensitivity, accuracy, flexibility, and speed. The constant progress in semiconductor manufacturing technology demands the fabrication, metrology, and control of ever smaller and more complex three-dimensional devices. Stacked nanosheet gate-all-around (GAA) devices will be the succeeding FinFET technology as the next-generation logic architecture in the coming years.[1-3] Complex integration schemes, specifically related to the gate definition, in conjunction with shrinking dimensions require precise process control for optimal device performance, which creates many new challenges for in-line metrology. One of the most critical manufacturing steps for GAA transistors is formation of inner spacers, which protect the channel from the source/drain regions during channel release. The first process step toward forming the inner spacer is a partial lateral etch of multiple sacrificial SiGe layers sandwiched in between epitaxial Si nanosheets, which are the electronic transport channels. Accurate, fast, and non-destructive measurements of the SiGe indentation etch are essential for competitive development and successful high-volume manufacturing. It is a demanding and challenging task for any metrology technique since the layers are vertically stacked and buried, and the nominal indents are only a few nanometers deep. Hence, the overall associated volume change is very small, leading to small metrology response changes. Ideally, a metrology accuracy of <1 nm is desired. The only suitable and currently available in-line metrology techniques for fully integrated samples are OCD, X-ray fluorescence (XRF), and maybe Raman spectroscopy.[4-7]

Previously published studies related to in-line metrology focused on the determination of the average sheet indent of simplified test structures[5,6] and fully integrated device architectures.[4] However, for the indent etch process, sheet-specific rather than single parameter monitoring is desired, because the process window for optimal device performance is very

small. If the indent is too deep or too shallow, the gate length will be too short or the spacer not thick enough to protect the source/drain regions, respectively. Monitoring an average indent depth only, multiple failure modes are possible that could go completely unnoticed. For example, in the case where the bottom sheet has a very shallow indent, the middle sheet exhibits a nominal indent depth, and the top sheet is too deep, the average indent of the three sheets could be on target but the device would fail due to an insufficient bottom spacer thickness. Therefore, sheet-specific indent monitoring is necessary for successful high-volume manufacturing. Scatterometry is currently the only available non-destructive in-line technique capable of sheet-specific monitoring of fully integrated wafers at relevant fin and gate pitches. Other techniques either lack the depth resolution, specifically when the dummy gate is present, or are destructive.

In this paper, SiGe indent monitoring capabilities for stacked nanosheet GAA device manufacturing using state-of-the-art OCD technology will be discussed. First, the latest advancement in scatterometry tool capabilities, Spectral Interferometry, is introduced and discussed. Then experimental strategies will be reviewed and highlighted that allow for monitoring an average indent with a goal of best time to solution. Furthermore, a straightforward methodology is described, which enables reproducible device manufacturing with engineered sheet-specific indent variations by tuning the alloy composition of the SiGe sheets individually. Lastly, sheet-specific indent results are presented and discussed. For both cases, monitoring the average SiGe indent or multiple sheet-specific indents, OCD enhanced with Spectral Interferometry improves the optical solution.

2. SPECTRAL INTERFEROMETRY

To provide adequate improvement of the metrology capabilities, OCD tools have gone through extensive improvement and refinement to allow extremely accurate measurements and high throughput. In addition to improving the essential tool characteristics, another venue by which OCD performance can be improved is diversifying the measured information. The majority of the current OCD solutions are based on well-established broadband spectral reflectometry and ellipsometry (SR/SE) techniques. These techniques are measuring the sample at different incidence angles, azimuths, polarizations, and wavelengths (Figure 1a).[8,9] Also, the relative phase between reflected polarization components can be accessed through ellipsometry measurements.

Another essential attribute of light scattered from a patterned structure is the phase difference between the incident and reflected electromagnetic waves (absolute spectral phase). Typically, this spectral phase has different values for different wavelengths, incident angles, azimuths, and polarizations and has new and unique information content. Since accessing the spectral phase directly is not possible at optical frequencies, one must use interference effects, usually observed with an interferometer, and recover the encoded phase information from the interference effects.

The difference between the relative and absolute spectral phase can be best illustrated with the Jones matrix, which describes the scattering of polarized light from samples.[8,9] The Jones matrix presents a light beam scattered from a sample by a 2-component complex vector, consisting of the amplitude and phase of each polarization (Jones vector $\vec{P}$). The polarization state will describe the scattered light (at a given azimuth and incidence angle): $\vec{P}' = J\vec{P}$. The Jones matrix is a 2×2 complex matrix of the form:

$$J = e^{i\varphi} \begin{pmatrix} r_{ss} & r_{sp} \\ r_{ps} & r_{pp} \end{pmatrix} \qquad (1)$$

Here, r_{ij} is the complex reflectance component for incident polarization j and scattered polarization i. For example, r_{ss} is the complex reflected field in the s polarization (perpendicular to the plane of incidence) when the incident field is s polarized. Similarly, r_{sp} represents the reflected s polarized field for incident field polarized in the p direction (parallel to the plane of incidence) and is related to the degree of polarization conversion created by the sample. The matrix components are complex and include relative phase difference between every two components, which is easily accessed through ellipsometry measurements and is different from the absolute spectral phase defined by the pre-factor $e^{i\varphi}$.

The Stokes-Mueller formalism, widely used for ellipsometry measurements, can be used as another example highlighting the difference.[8,9] For non-depolarizing samples, there is a simple transformation between the Jones and Stokes-Mueller matrices: $M = TJJ^*T^{-1}$, where M is a Mueller matrix, and T is the conversion matrix:

$$T = \begin{pmatrix} 1 & 0 & 0 & 1 \\ 1 & 0 & 0 & -1 \\ 0 & 1 & 1 & 0 \\ 0 & i & -i & 0 \end{pmatrix} \qquad (2)$$

Transformation shows that for the non-depolarizing samples, the Mueller matrix does not hold any additional information content not included in the Jones matrix. On the other hand, the Jones absolute phase component vanishes in conversion, so in the Mueller matrix formalism the absolute spectral phase is not present.

In this paper, the enhanced OCD hardware is presented. It combines multichannel reflectivity measurements with measurements of the absolute spectral phase. The optical scheme of the Spectral Interferometer (SI) is depicted in Figure 1b. It is based on a Spectral Reflectometer, where sample reflectivity is accurately measured. However, in this scheme, the objective lens used for the measurement is replaced by an interferometric objective. Optical path difference control can be obtained by changing either the sample arm's length or modifying the reference arm path. Light from the reference mirror and the sample are combined in the beam splitter and directed to the spectrometer. The spectrometer measures the intensity of every wavelength separately and records the interference pattern of the interferometer. The unique design must ensure the required stability of interferometric measurements to external noise sources and enable fast throughput for high-volume manufacturing environments.

We present the enhanced OCD hardware capabilities, enabling measurement of reflectivity and absolute spectral phase, for one of the most challenging applications of future nanosheet technology – sheet-specific indent metrology.
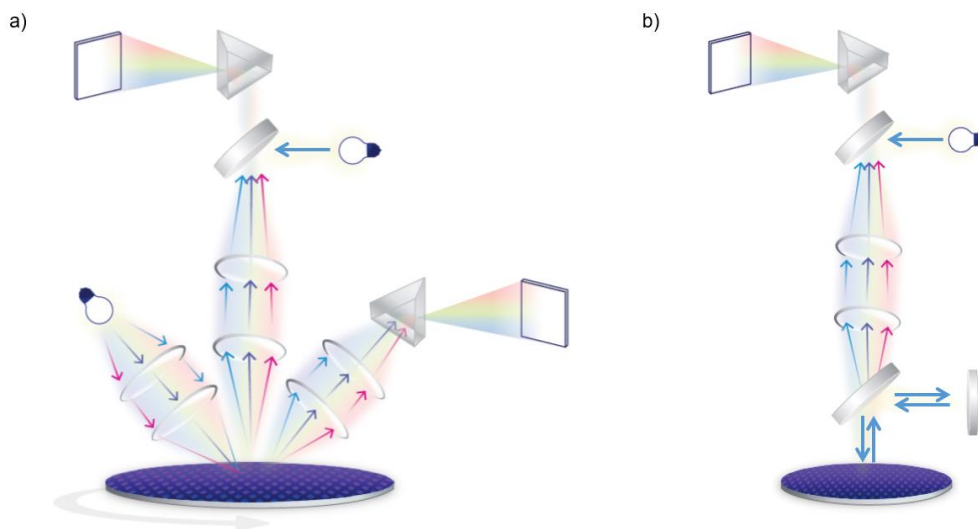
Figure 1. (a) Schematic of current multichannel OCD tools, including normal incidence and oblique illumination and collection channels. (b) Schematic of Spectral Interferometer (SI): light is split between the sample and a reference arm and then recombined and measured with a spectrometer.

3. DESIGN OF EXPERIMENTS

3.1 Single Parameter Indent Monitoring

Single indent parameter monitoring refers to the characteristic that the optical metrology solution is capable of delivering a single value corresponding to the average indentation of all SiGe sheets. In this study, the GAA device comprises a nanosheet stack with three epitaxial SiGe sheets sandwiched between thin epitaxial Si layers. Fully integrated wafers were processed with nominal conditions up to the lateral SiGe etch. At the SiGe indent process step, an intentional variation using five different etch times was introduced with the goal to change the indent of all three sheets equally from shallow

to deep. All wafers were measured with advanced multichannel scatterometry (T600MMSR and NovaPRISM) after indentation as well as with low energy XRF (VeraFlexIII+) before and after indentation. Center and edge scanning transmission electron microscopy (STEM) images from each wafer were obtained to evaluate the etch variations and serve as reference for the optical model solution.

The optical solution comprises a full geometric model with many degrees of freedom to account for potential process variations. Additionally, a machine learning solution was developed using scatterometry in conjunction with XRF reference data.[4]
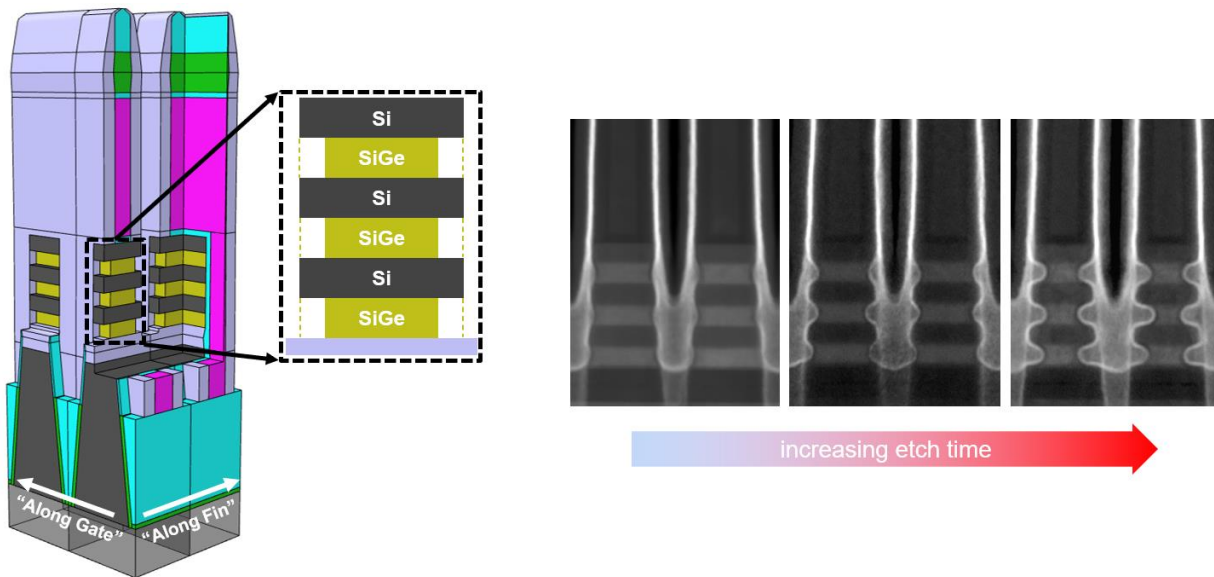
Figure 2. Full geometric optical model developed for single parameter indent monitoring; the inset shows a more detailed view of the nanosheet stack comprising alternating epitaxial Si and SiGe layers. STEM cross-section images with cuts perpendicular to the gate direction depict three of the five etch conditions with successive increase in SiGe indentation from left to right.

3.2 Individual Sheet Indent Monitoring

Individual sheet indent monitoring refers to the characteristic that the optical metrology solution is capable of delivering a single indent parameter for each of the multiple SiGe layers within the nanosheet stack. For the individual sheet indent monitoring part of the study, wafers with fin patterning only have been considered. Nonetheless, considering the small volume change per layer and the fact that there are multiple instances of alternating thin Si and SiGe sheets, the question of metrology sensitivity arises first. Figure 3 shows spectral sensitivity calculations for a bottom, middle, and top sheet variation of 2 nm, respectively, at otherwise constant geometry. Representative MMSR channels at normal and oblique angles of incidence confirm that the optical fingerprint differences between the three individual sheet variations are significant and significantly different from each other. The SI channel adds additional unique spectral sensitivity. Therefore, an appropriate optical model will be capable of discriminating between the individual sheets and can deliver sheet-specific indent monitoring.

In order to experimentally evaluate and confirm the calculated sheet-specific capabilities and develop a reliable metrology solution, a set of samples with certain properties is desired. Ideally, the indent variations can be precisely and reproducibly controlled, individually by sheet and decoupled from any other potential process variations. Desired samples include, for example, a successive increase or decrease from top to bottom, and a set where two sheets are processed nominally while a third sheet has a deeper (or shallower) indent – and this sheet is then intentionally the top, middle, or bottom sheet. Furthermore, reliable reference metrology besides STEM cross-section images is desired that is non-destructive, less expensive, and less sensitive to potential local variability.
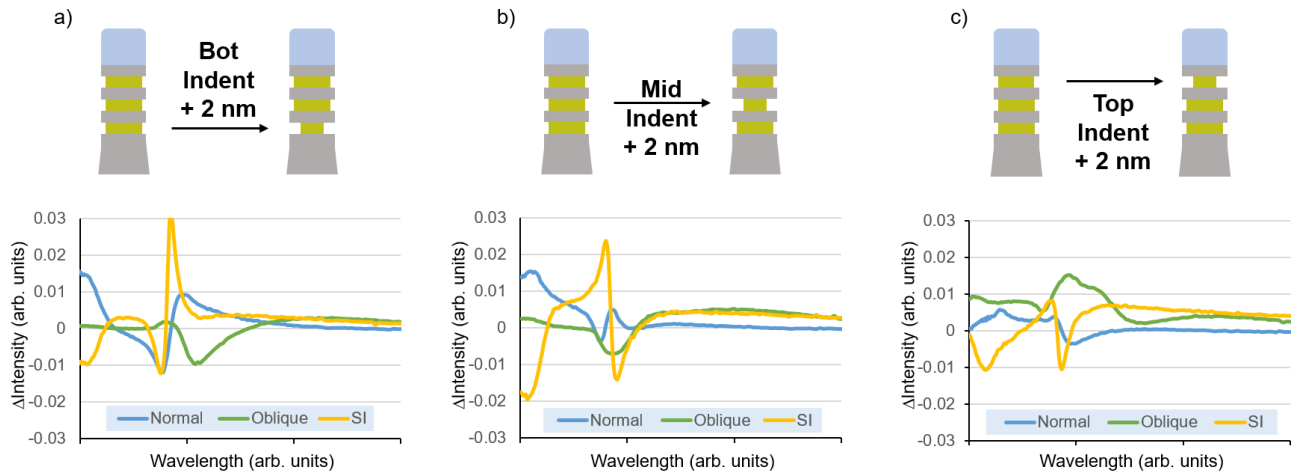
Figure 3. Spectral sensitivity calculations for sheet-specific indent variations. Shown are schematics of the top portion of a fin with multilayer Si/SiGe nanosheet stack with (a) bottom, (b) middle, and (c) top sheet variations of 2 nm together with respective unique optical fingerprint differences for representative Normal (blue), Oblique (green), and SI (yellow) optical channels.

Unfortunately, the etch process employed for the SiGe indentation itself does not allow for such a controlled sheet-specific variability. However, the etch rate strongly depends on the Ge content within the SiGe alloy.[10] The composition of the SiGe alloy can be very well controlled for each sheet at nanosheet stack epitaxy. Hence, a small sheet-specific variation of the Ge content at otherwise nominal process conditions will allow for the desired sheet-specific indent control and a reproducible manufacturing.

The samples manufactured for this study are listed in Table 1. No intentional process variations other than the sheet-specific Ge concentration were introduced. The range was selected such that the dependency of etch rate versus Ge content is linear and that the high Ge content sheet etches about two times faster compared to the sheet with the low Ge content. All samples were measured by high-resolution X-ray diffraction (HRXRD) post nanosheet stack deposition to determine individual sheet thickness and desired Ge content variations.[7] Additionally, low energy XRF measurements were carried out before and after the indentation to measure Ge Lα counts, which are representative of the total amount of Ge present within the probed volume.

Table 1. List of samples with sheet-specific Ge content variations from low (L), medium (M) and high (H).

Slot	Bottom	Middle	Top	Group
1	H	M	L	
2	L	M	H	Successive In/Decrease
3	L	M	H	
4	M	L	L	
5	L	M	L	One Sheet More (M)
6	L	L	M	
7	L	M	M	
8	M	L	M	One Sheet Less
9	M	M	L	
10	H	L	L	One Sheet More (H)
11	L	L	H	

Figure 4 depicts STEM cross-section images and indent measurements of slots 3 and 6. Slot 3 represents a sample with successive increase in Ge content going from bottom to top sheet and the STEM image results are a testament that the

processing worked as intended. The sheet-specific indent measurements show an approximately 4, 6.5, and 9 nm indentation on each side for the bottom, middle, and top sheets, respectively. Hence, the etch rate as a function of Ge content exhibits a linear behavior where the sheet with higher Ge concentration etches a little over two times faster compared to the sheet with the low Ge content. Slot 6 is a sample from the group 'one sheet more' and helps to confirm that the indent only depends on the Ge content and is independent of the location of the sheet. Both bottom and middle sheets are epitaxially grown with the same low Ge concentration. Consequently, the indent measurements are with around 4 nm essentially identical as well as in excellent agreement with the indent of the low Ge content sheet of slot 3. The two M sheet measurements do not match as well as the one for the L sheets, which is likely related to process variations and image analyses uncertainty.
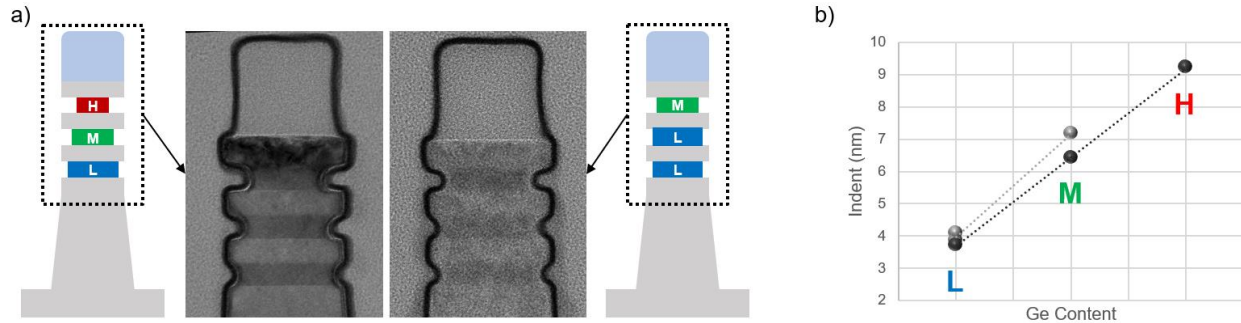
Figure 4. Representative STEM cross-sections of (a) slots 3 (left) and 6 (right) together with (b) sheet-specific indent measurements of these two samples as a function of Ge content. The topmost layer in (a) is a hardmask required for patterning.

Regarding the former, it has been discussed that the SiGe etch rate depends on the Ge content, the basic concept of the entire sheet-specific design of experiments. Assuming process variations with a Ge content range of ±0.05 around the target value, at the process conditions used for this study, an indent variation of already ±2.4 Å can be expected. Furthermore, the indent etch rate also scales with sheet height. Assuming a sheet-to-sheet height variation of ±5 Å, depending on the alloy composition an indent range of ±2.2 and ±5.2 Å and for the low and high Ge content sheets, respectively, can be expected. Hence, in the worst-case scenarios (upper and lower bounds) the indentation of sheets with a low Ge content may be different by over 9 Å due to processing variations. Additionally, STEM image analyses results carry an error due to the image calibration and manual readout, sometimes exacerbated by imaging artefacts, and represent only a small slice of the target without depth information.
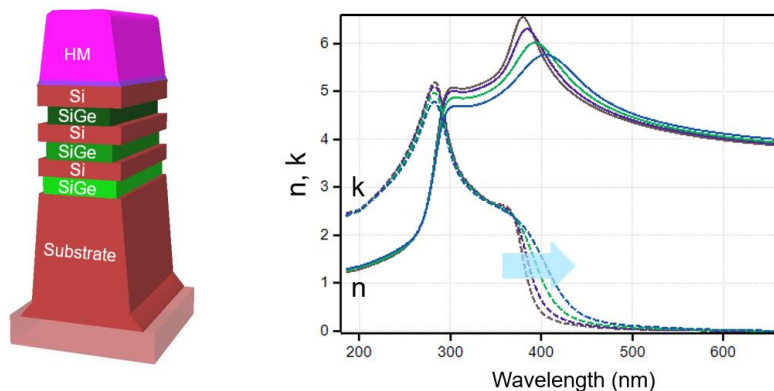
Figure 5. Optical model for sheet-specific indent monitoring with hardmask (HM), Si and SiGe layers, and Si substrate (left); and SiGe optical properties, refractive index n and extinction coefficient k, with varying Ge content (right). The arrow indicates the red-shift as the alloy becomes more germanium-rich.

The optical model required for the patterned and indented nanosheet stack wafers (Table 1) is reasonably straightforward. Besides the individually parameterized sheets, the overall fin and hardmask geometries need to be accounted for. Additionally, since the design of experiments is based on a variation of the Ge content, the optical properties (n and k) of the SiGe alloy have to be considered as they depend on the specific alloy composition (Figure 5). It was confirmed, by way of simulations, that there is no significant correlation between SiGe composition and the indent itself. Specifically, a change in the Ge content causes a different optical fingerprint change than the indent does.

4. RESULTS AND DISCUSSION

4.1 Single Parameter Indent Monitoring

The main challenge with a geometric model for fully integrated devices and stand-alone indent monitoring (analyzing a single measurement only acquired post indentation) is the many floating parameters required to account for process variations within the fin and gate module. Hence, there is a risk that the model accuracy lacks due to parameter correlations, especially since the etched SiGe volume is very small, or non-unique solutions can be found. Nonetheless, the match between indent values reported by the OCD model for the five different etch conditions is in good agreement with STEM cross-section image analyses (Figure 6a). In this example, adding SI channels improves the correlation to STEM from $R^2 = 0.8$ with MMSR channels only to the depicted $R^2 = 0.9$.[4]

While this is an excellent result, another challenge is to keep metrology up to date, especially in the development stage of a manufacturing process. Meaning, a full geometric model may need to be revised because of a small process change somewhere upstream in the line. Time to solution is critical and building an OCD solution based on a full geometric model including the calculation of a new model library is typically time consuming. To improve time to solution significantly and be less dependent on process variations unrelated to the indent itself, a machine learning solution utilizing XRF as a reference was developed. Specifically, the difference in Ge Lα (ΔGe) counts between before and after indentation, which represents the overall loss of Ge, was used to train a machine learning model with scatterometry spectra acquired after indentation only. Figure 6c depicts the excellent correlation between normalized ΔGe counts and OCD machine learning results achieved already with only a few data points. Subsequently, only a few representative STEM reference images are required to convert ΔGe counts to an indent depth in nanometers. This type of machine learning approach is basically effortless compared to a full geometric model build because it only requires two XRF reference measurements from a few wafers to get started. The time to solution in case an update is required can be counted in minutes rather than days with the right infrastructures in place.[11]
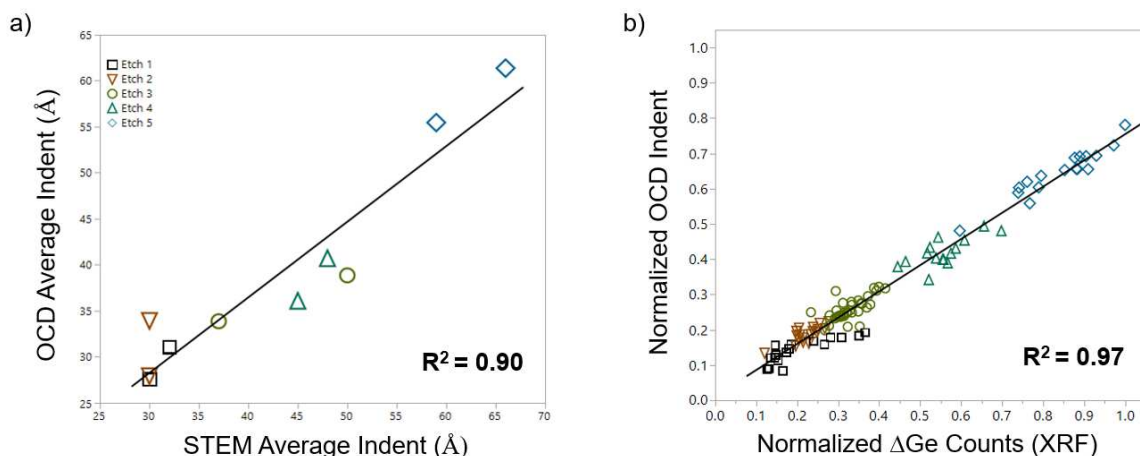
Figure 6. Correlation plots of (a) STEM and OCD results from the full geometric model using MMSR+SI channels and (b) normalized ΔGe counts and OCD indent values as obtained by a machine learning solution using XRF reference data.

4.2 Individual Sheet Indent Monitoring

The sheet-specific SiGe indent scatterometry results for all eleven wafers listed in Table 1 are presented in Figure 7. The graphs are vertically separated in three sections representing indent results for bottom, middle, and top sheet. Within each section the *y*-axis lists the slots in ascending order and the common *x*-axis shows the indent in units of angstroms. The size of the box and whiskers indicates the data spread of ten measurements across the wafer and the color designates the Ge content low (blue), medium (green), and high (red). The three vertical grey areas around 35, 65 and 95 Å are guides to the eye.

Figure 7a depicts best model indent data from fitting MMSR and SI channels and the red circles are the STEM data from two wafers (see Figure 5). Focusing first on slot 3, it is evident that OCD matches the STEM data very well for all three sheets: the bottom sheet with the lowest Ge content is indented by about 40 Å, the middle sheet with the medium concentration around 75 Å, and the germanium-rich top sheet is indented the most with 90 Å. In a similar manner, STEM data matches well with the OCD model output for slot 6. However, looking at all results for low Ge content sheets (blue boxes around 35 Å) for example, a median range of >10 Å is observed, and it looks like the bottom sheets tend to have deeper indents than the top sheets, for instance. The obvious first suspicion is that there are parameter correlations in the optical model, either between sheets or with other floating geometrical parameters. Thorough analyses did not confirm that there are significant correlations between any of the floating model parameters. Hence, the variations should be mainly related to processing.
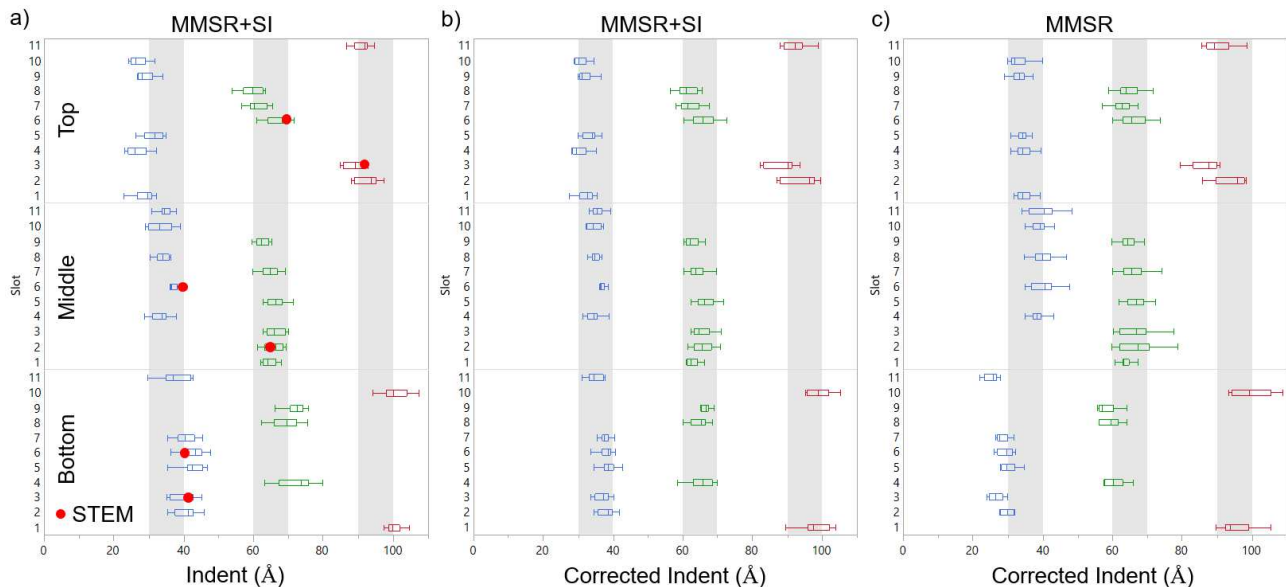
Figure 7. Sheet-specific SiGe indent scatterometry results for all eleven wafers listed in Table 1 vertically separated by sheet location (bottom, middle, top). The color of the boxes represents the Ge content of the sheets: low = blue, medium = green, and high = red. (a) OCD model results considering MMSR and SI channels; XRD "sheet factor" corrected OCD model results considering (b) MMSR and SI channels and (c) MMSR channels only.

In an attempt to verify if processing variations are the major source of variations here, sheet-specific heights and Ge contents, as determined by HRXRD at the blanket stage were used to calculate a location-specific "sheet factor" proportional to the etch rate. For example, sheets with a high sheet factor are expected to etch faster because they have an above nominal height and/or Ge content. This scaling factor is then applied to the reported OCD indent values and results are shown in Figure 7b. It is evident that the corrected indent results, specifically for the sheets with low and medium Ge content, have "improved" in terms of data spread. These results give confidence that a significant part of the data spread is indeed related to process variations at nanosheet stack epitaxy rather than issues with the OCD metrology or the model. The remaining variation is attributed to the data correction procedure and total measurement uncertainties for both HRXRD and OCD. The HRXRD data correction procedure to determine the location-specific "sheet factor" in this study is not

optimal since the OCD and HRXRD sampling plans do not match exactly. Therefore, with the assumption of radial symmetry, OCD indent results were corrected with data from close radial neighbors. It is believed that an improvement is possible with matching sampling plans and maybe additional reference metrology using x-ray reflectometry, for example.

In summary, the claim is not that OCD indent results must be corrected to get an accurate reading, but that the original and uncorrected results (Figure 7a) are in fact accurate. Small process variations at multilayer stack epitaxy rather than OCD metrology or model issues are likely the main source of variation. Therefore, the epitaxial SiGe deposition process needs to be controlled with extreme precision and accuracy to achieve even indents.

If the unique information content obtained from SI channels is not considered for the model analysis, the results are still acceptable but not as robust (Figure 7c). For ease of comparison, the corrected indent is shown. A slightly larger deviation from the median within the population is observed. Besides that, it stands out that specifically the low Ge content bottom sheets are on average about 5-10 Å below expectation.
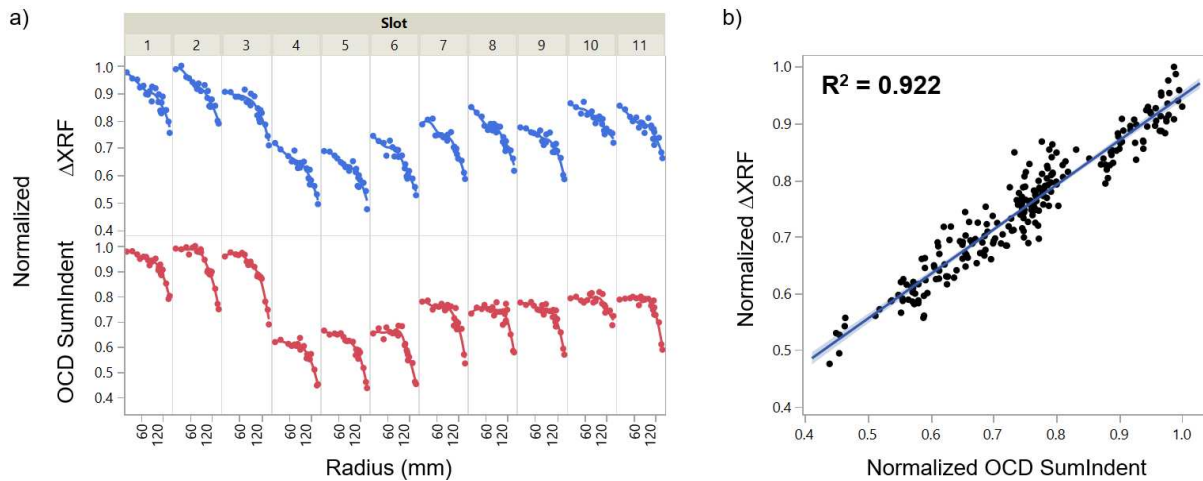
Figure 8. Comparison between XRF and OCD (a) as a function of radius per slot and (b) a combined correlation plot.

In addition to STEM image analyses and working with sheet-specific HRXRD data, the OCD indent results are compared to XRF reference data. Ge Lα counts were measured on all OCD measured sites before and after the SiGe indent etch. While not a sheet-specific metric, the difference between these two acquisitions is representative of the total amount of Ge removed during the etch process (ΔXRF = GeLα_{pre} – GeLα_{post}). In order to compare both XRF and OCD metrology results, the sheet-specific OCD indent parameters are multiplied with the respective Ge content to yield an empirical SumIndent parameter according to

$$\text{OCD SumIndent} = (\text{Indent*Ge\%})_{Bot} + (\text{Indent*Ge\%})_{Mid} + (\text{Indent*Ge\%})_{Top} . \tag{3}$$

A comparison between ΔXRF and OCD SumIndent is presented in Figure 8. The graph is horizontally separated by the wafers and the x-axis within each panel depicts the wafer radius (Figure 8a). It is noticeable that both techniques report a considerable difference between center and edge. Additionally, based on the amplitude, the wafers can be separated into three groups based on the total Ge content matching the experiment: slots 1…3 have the highest and slots 4…6 the lowest values; the other four wafers are in between. In general, the ΔXRF (top row) and OCD SumIndent (bottom row) are matching well in terms of amplitude and radial signature, which is also confirmed by the combined correlation plot with $R^2 = 0.92$ (Figure 8b).

5. CONCLUSIONS

In this paper, SI technology, which allows for the temporal characterization of the wavefront by measuring the absolute phase through spectral interferometry was introduced and discussed. Spectral Interferometry adds additional and unique

sample information, which enhances existing scatterometry capabilities and supports solving the most challenging applications. It was shown how the addition of spectral phase information acquired by SI improved the presented optical metrology solutions around SiGe indent metrology within the inner spacer module of gate-all-around nanosheet device manufacturing.

Single indent parameter monitoring solutions were presented and summarized. A geometric model utilizing MMSR and SI technology for in-line monitoring of fully integrated devices can deliver very good average indent results as confirmed by STEM reference data. However, maintaining such a model in the development stage of a process with all its minor or major adjustments is time-consuming and hence expensive. It was highlighted how a machine learning model trained with XRF reference data could easily replace the full geometric model. In a straightforward manner excellent results can be achieved with only a few wafers of training data.

Lastly, a methodology was introduced and discussed that allows for reliable and reproducible manufacturing of reference samples with sheet-specific indent variations, which can be used to evaluate optical model solutions. Minor intentional variations of the Ge content within individual SiGe nanosheets allow for engineered etch differences without modifying the nominal etch process. It was demonstrated that an OCD model utilizing information from SI channels is capable of delivering excellent sheet-specific results. While the data presented here are for structures without gates, the introduced concept can be readily applied to design experiments for fully integrated flows. The results presented here highlight that minor process variations in terms of sheet height and alloy composition can affect the indent depth substantially. Therefore, epitaxial growth monitoring and tight process control are crucial for reliable indent manufacturing. XRD and XRF data were used to confirm the accuracy of the OCD model.

6. ACKNOWLEDGEMENTS

REFERENCES

[1] M. Lapedus, "New Transistor Structures At 3nm/2nm," 25 January 2021, <https://semiengineering.com/new-transistor-structures-at-3nm-2nm/> (02 February 2021).
[2] N. Loubet, T. Hook, P. Montanini, C.-W. Yeung, S. Kanakasabapathy, M. Guillom, T. Yamashita, J. Zhang, X. Miao, J. Wang, A. Young, R. Chao, M. Kang, Z. Liu, S. Fan, B. Hamieh, S. Sieg, Y. Mignot, W. Xu, S.-C. Seo, J. Yoo, S. Mochizuki, M. Sankarapandian, O. Kwon, A. Carr, A. Greene, Y. Park, J. Frougier, R. Galatage, R. Bao, J. Shearer, R. Conti, H. Song, D. Lee, D. Kong, Y. Xu, A. Arceo, Z. Bi, P. Xu, R. Muthinti, J. Li, R. Wong, D. Brown, P. Oldiges, R. Robison, J. Arnold, N. Felix, S. Skordas, J. Gaudiello, T. Standaert, H. Jagannathan, D. Corliss, M.-H. Na, A. Knorr, T. Wu, D. Gupta, S. Lian, R. Divakaruni, T. Gow, C. Labelle, S. Lee, V. Paruchuri, H. Bu, M. Khare, "Stacked Nanosheet Gate-All-Around Transistor to Enable Scaling Beyond FinFET," Symp. VLSI Tech., 230–231 (2017).
[3] J. Zhang, J. Frougier, A. Greene, X. Miao, L. Yu, R. Vega, P. Montanini, C. Durfee, A. Gaul, S. Pancharatnam, C. Adams, H. Wu, H. Zhou, T. Shen, R. Xie, M. Sankarapandian, J. Wang, K. Watanabe, R. Bao, X. Liu, C. Park, H. Shobha, P. Joseph, D. Kong, A. Arceo De La Pena, J. Li, R. Conti, D. Dechene, N. Loubet, R. Chao, T. Yamashita, R. Robison, V. Basker, K. Zhao, D. Guo, B. Haran, R. Divakaruni, H. Bu, "Full Bottom Dielectric Isolation to Enable Stacked Nanosheet Transistor for Low Power and High Performance Applications", 2019 IEEE International Electron Devices Meeting (IEDM).
[4] D. Kong, D. Schmidt, M. Breton, J. Frougier, A. Greene, J. Zhang, V. Basker, N. Loubet, I. Ahsan, A. Cepler, M. Klare, M. Cheng, R. Koret, I. Turovets, "Development of SiGe Indentation Process Control to Enable Stacked Nanosheet FET Technology," 2020 31st Annual SEMI Advanced Semiconductor Manufacturing Conference (ASMC).
[5] M. Korde, S. Kal, C. Alix, N. Keller, G.A. Antonelli, A. Mosden, A.C. Diebold, "Nondestructive characterization of nanoscale subsurface features fabricated by selective etching of multilayered nanowire test structures using Mueller matrix spectroscopic ellipsometry based scatterometry," J. Vac. Sci. Technol. B 38, 024007 (2020).

[6] J. Bogdanowicz, Y. Oniki, K. Kenis, Y. Muraki, T. Nuytten, S. Sergeant, A. Franquet, V. Spampinato, T. Conard, I. Hoflijk, J. Meersschaut, N. Claessens, A. Moussa, D. Van Den Heuvel, J. Hung, R. Koret, A.-L. Charley, P. Leray, "Spectroscopy: a new route towards critical-dimension metrology of the cavity etch of nanosheet transistors," Proc. SPIE 11611, 116111Q (2021).

[7] D. Schmidt, C. Durfee, J. Li, N. Loubet, A. Cepler, L. Neeman, N. Meir, J. Ofek, Y. Oren, D. Fishman, "In-Line Raman Spectroscopy for Stacked Nanosheet Device Manufacturing," Proc. SPIE 11611, 116111T (2021).

[8] R.M.A. Azzam, "Mueller-matrix ellipsometry: a review,", Proc. SPIE 3121 (1997).

[9] D. Shafir, G. Barak, M.H. Yachini, M. Sendelbach, C. Bozdog, S. Wolfling, "Mueller matrix characterization using spectral reflectometry", Proc. of SPIE 8789 (2013).

[10] B. Holländer, D. Buca, S. Mantl, J. M. Hartmann, "Wet Chemical Etching of Si, $Si_{1-x}Ge_x$, and Ge in HF:H2O2:CH3COOH," J. Electrochem. Soc., 157, H643 (2010).

[11] P. Timoney, R. Luthra, A. Elia, H. Liu, P. Isbester, A. Levy, M. Shifrin, B. Bringoltz, E. Rabinovich, A. Broitman, E. Rothstein, R.Yacoby, I. Rubinovich, Y.H. Kim, O. Shlagman, B. Ben-Nahum, M. Zolkin, Igor Turovets, "Advanced machine learning eco-system to address HVM optical metrology requirements," Proc. SPIE 11325, 113251H (2020).